

# Single Beacon Acoustic for AUV Navigation

P. Baccou, B. Jouvencel, V. Creuze

baccou@lirmm.fr, jouvence@lirmm.fr, creuze@lirmm.fr

LIRMM

161, rue Ada

34392 Montpellier cedex 5

France

## Abstract

*This paper presents an algorithm allowing an AUV to determine its position with respect to a beacon by ranging to that beacon. The beacon's absolute position is known onboard the AUV so that the relative position can be converted into an absolute position. The major difficulty of this approach is that a single range measurement does not completely constrain the vehicle's relative position. The AUV then has to ping the beacon from different places, while measuring its displacements between pings, in order to triangulate its position. Since the AUV can initially have a very approximate knowledge of its own absolute position, the navigation procedure is divided into three phases. The first step consists of obtaining an initial estimate of the vehicle's absolute position and of the disturbances affecting the quality of the dead reckoned displacements (underwater components and speed bias). The second step consists of refining the position and the disturbance estimates by navigating with respect to the beacon so as to maximize the information matrix. Finally, the third step consists of the actual survey during which the AUV keeps ranging to the beacon to maintain an accurate absolute position.*

## 1. INTRODUCTION

Long baseline navigation systems have been used for several decades [1] for the positioning of underwater equipment and manned submersibles, and more recently for the navigation of Autonomous Underwater Vehicles [2][3][4][5]. Although, these systems can offer a good positioning accuracy, provided the array is correctly calibrated, they also have several drawbacks. The deployment and the recovery of the transponders as well as the calibration of the array are ship-time consuming and therefore expensive. Furthermore, the whole process has to be repeated each time the array is moved to a different place. The overall cost of the system is also substantial given the cost of each beacon.

Therefore, a different approach consisting of using a single beacon is being studied [6][7][8]. The advantage of such a solution is that the calibration reduces to the determination of the beacon's location. Whereas the vehicle track is distorted by errors on the baseline calibration in the classical long

baseline approach, any beacon position calibration error results in a shift of the AUV position equal to the calibration error in the single beacon approach. This approach could appear very attractive at first sight. It has, however, an important disadvantage associated with the fact that it is not possible to determine the vehicle's position from a single ping. In classical long baseline navigation, the replies to a single ping can be used to triangulate the AUV's position (provided the number of returns is sufficient and the measured ranges are valid). With a single beacon, the AUV has to ping the beacon from different places in order to triangulate its position. The baselines between ranges are then created by the displacements of the AUV, which have to be measured with maximal accuracy. As opposed to the solution presented in [8], which relies on an accurate dead reckoning system to measure the displacements, our concern is to provide a solution for vehicles equipped with low-cost sensors. The availability of a Doppler velocity log is then not an option due to the sensor's cost, and we rather consider that the vehicle's speed is approximately known by a priori calibration of the vehicle's water speed as a function of propeller rpm. At this point, however, we consider that the vehicle has a reliable heading reference, but we are currently studying modifications of the algorithm to remove this restriction. The vehicle's speed, used in the computation of the displacements, is then affected by a bias due to speed vs. rpm calibration errors and by the unknown underwater current components. These error sources will be estimated together with the vehicle's position.

The beacon's absolute position is known by the AUV, but in many cases the AUV will only approximately know its own initial absolute position. This is the case if the AUV has to dive deep after a surface GPS fix, or if it has traveled for a long time underwater before getting within range of the beacon. For this reason, we will assume that the AUV has no knowledge of its initial absolute position. The first step then consists of obtaining an estimate of the AUV's absolute position by having the AUV describe a circle while ranging to the beacon and dead reckoning its displacements between ranges. A least squares optimization is then applied to the data resulting in an initial estimate of the AUV's absolute position and initial estimates for the speed bias and the underwater current components. To reduce the uncertainty on these estimates and obtain an accurate absolute position before beginning the survey, the AUV runs a Kalman filter taking round-trip travel times as observations and estimating the AUV's position and the disturbances. The vehicle travels so as to maximize the information matrix until the estimation

error covariance has sufficiently reduced. The AUV then start its survey in good conditions and follow its desired survey trajectory. The positioning during the survey is performed by the same Kalman filter.

The paper is organized as follows: section II defines important reference frame. Section III describes the initialization procedure allowing to obtain the initial state estimate and its error covariance matrix used to initialize the Kalman filter. Section IV describes the Kalman filter in details and particularly how the vehicle's motion between ping and reply is taken into account. Section V describes how the position estimate is improved thanks to the information matrix. Section VI presents simulation results.

## 2. DEFINITIONS

The location of the beacon in the local absolute reference frame  $R_0$  is  $(x_b, y_b, z_b)$ . This location is known by the AUV. The axes  $x_0$  and  $y_0$  respectively point north and east, and  $z_0$  points down. The mobile frame  $R_m$  is located at the center of gravity of the vehicle with its axes  $x_m, y_m, z_m$  parallel to  $x_0, y_0, z_0$ . The knowledge of the beacon's depth allows to convert the 3D problem into a 2D problem. The terminology 'range' in the remaining of the paper should then be understood as x-y range (slant range corrected for the depth difference between the vehicle and the beacon). The acoustic travel times are measured like in a Long Base Line system: the vehicle pings, the beacon replies upon reception after a given timeout and the vehicle detects the time of arrival of the reply. Slant ranges are calculated based on the known average speed of sound.

## 3. INITIALIZATION

### 3.1. Principle

The initialization of the beacon's location consists of commanding a 360° rotation to the AUV while ranging to the beacon and measuring the displacements between pings (Fig.1). The vehicle would thus describe a circular path in the absence of underwater current or a distorted circle otherwise.

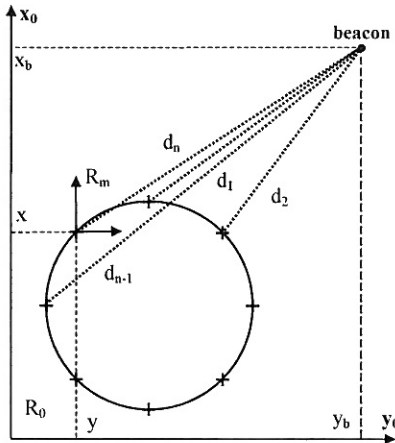


Fig. 1: Geometry of the initialization procedure

In the presence of a speed bias ( $du$ ) and of an underwater current ( $v_{cn}, v_{ce}$ ) all assumed to be constant, the north and east components of the vehicle's displacement over a sampling period  $\Delta t$  can be modeled by:

$$\begin{cases} \Delta x = C\theta C\psi(u-du)\Delta t + v_{cn}\Delta t \\ \Delta y = C\theta S\psi(u-du)\Delta t + v_{ce}\Delta t \end{cases} \quad (1)$$

Where  $u$  is the vehicle's calibrated water referenced speed,  $\theta$  is pitch and  $\psi$  its heading.  $C\theta, S\theta, C\psi, S\psi$  are  $\cos(\theta), \sin(\theta), \cos(\psi), \sin(\psi)$  abbreviations.

The displacements between ranges  $i$  and  $n$  can then be written:

$$\begin{cases} \Delta x_{i,n} = \sum_{k=i}^{k=n} C\theta_k C\psi_k u_k \Delta t - du \sum_{k=i}^{k=n} C\theta_k C\psi_k \Delta t + v_{cn} \sum_{k=i}^{k=n} \Delta t \\ \Delta y_{i,n} = \sum_{k=i}^{k=n} C\theta_k S\psi_k u_k \Delta t - du \sum_{k=i}^{k=n} C\theta_k S\psi_k \Delta t + v_{ce} \sum_{k=i}^{k=n} \Delta t \end{cases} \quad (2)$$

Let  $R_m$  be the mobile frame at the time  $d_n$  is measured (end of the rotation) and  $(x, y)$  be the vehicle's absolute position at that time. The  $i^{\text{th}}$  range can be expressed as a function of the vehicle's position at the end of the rotation and of the displacement between ranges  $i$  and  $n$  by:

$$d_i = \left[ (x_b - x + \Delta x_{i,n})^2 + (y_b - y + \Delta y_{i,n})^2 \right]^{1/2} \quad (3)$$

The system of equations (3) can be solved for  $(x, y, du, v_{cn}, v_{ce})$  by non-linear least squares using the Levenberg-Marquardt algorithm. However, because the problem can have local minima, we could not initialize the search with  $(0, 0, 0, 0, 0)$  without risking convergence to an erroneous solution. Therefore, in order to initialize closer to the correct solution, the system without current or speed bias is first solved starting at  $(x, y) = (0, 0)$ . The approximate vehicle position obtained in that case is then used to initiate the search in the presence of current (the current components and the bias being still initialized at 0).

### 3.2. Range pre-processing

In our simulations, we chose to use a selection of 14 ranges for the estimation of  $(x, y, du, v_{cn}, v_{ce})$ . Since ranges can sometimes be spurious because of noise or multi path, the 14 ranges have to be selected carefully. The set of ranges is first pre-filtered as follows: the difference between successive ranges is computed and a threshold is applied. If the difference is greater than the threshold, further testing is performed by looking at the ranges before and after the considered pair. Depending on the results of these additional tests, either both ranges are discarded or only one.

A median method is then applied to the remaining ranges:

- Select 14 ranges randomly (depends on the noise and on the number of ranges),
- Compute the solution to equation (3),
- Characterize the solution with the median of the range residuals.

Repeat these steps  $N$  times and keep the set of 14 ranges providing the smallest median residual.

N has to be chosen even larger that the range measurements are noisy. This is of course at the expense of a longer computation time. For the simulations, we used N=70 (it's because of the greatest of the ranges noises: 20% are spurious and 20% are affected by a Gaussian noise). We can use N=30 for 10% of spurious ranges and 15% with a Gaussian noise.

### 3.3. Uncertainty on the initial estimation

The system of equations (3) can be expressed by:

$$d = f(X, \psi, \theta, u, \Delta t) + n \quad (4)$$

Where d is the vector of the selected ranges,  $X=(x,y,v_{cn},v_{ce},du)^t$ , and n is a Gaussian noise on the measured ranges with variance matrix R. The non-linear least squares optimization provides the covariance matrix of X (Cramer-Rao lower bound):

$$P = \left[ \left( \frac{\partial f(X)}{\partial X} \right)' (HP_e H_t + R)^{-1} \left( \frac{\partial f(X)}{\partial X} \right) \right]^{-1} \quad (5)$$

Where H is the Jacobian of the ranges with respect to  $\psi, \theta, u$  and  $P_e$  is the covariance matrix of  $\psi, \theta, u$ . The result of the optimization is used to initialize the state vector of the Kalman filter described below, and the covariance matrix P is used to initialize the estimation error covariance matrix of the filter.

## 4. EXTENDED KALMAN FILTER

### 4.1. State equation

The state vector is made up of the vehicle's position (x,y) in  $R_0$ , the vehicle's depth (z), the components of the underwater current ( $v_{cn}, v_{ce}$ ) and the speed bias (du). The inputs are the vehicle's heading  $\psi$ , its pitch  $\theta$  and its water-referenced speed u. The covariance matrix of the inputs is the diagonal matrix  $C_{in} = \text{diag}(\sigma_\psi^2, \sigma_\theta^2, \sigma_u^2)$ . The current and the speed bias are modeled as constant. The state noise vector is  $v_k$  and its covariance matrix  $Q_k$ . The state equation is then expressed by:

$$\begin{bmatrix} x \\ y \\ z \\ v_{cn} \\ v_{ce} \\ du \end{bmatrix}_{k+1} = \begin{bmatrix} x \\ y \\ z \\ v_{cn} \\ v_{ce} \\ du \end{bmatrix}_k + \begin{bmatrix} C\theta C\psi(u-du) + v_{cn} \\ C\theta S\psi(u-du) + v_{ce} \\ -S\theta(u-du) \\ 0 \\ 0 \\ 0 \end{bmatrix} \Delta t + v_k \quad (6)$$

### 4.2. Observation equation

The observation equation expresses the acoustic round-trip time of flight (T) as a function of the vehicle's state at the time of the ping and at the time the vehicle receives the reply from the beacon. The vehicle's motion between the ping and

the reception is then taken into account, and the observations are expressed in terms of all the state variables. The measurement noise on the travel times is represented by  $w_k$ . Its variance is  $R_k$ . The speed of sound is noted c and the beacon turn around time  $\Delta t_r$ .

$$T = \frac{1}{c} \left\{ \left[ (x_b - \hat{x}_{ping})^2 + (y_b - \hat{y}_{ping})^2 + (z_b - \hat{z}_{ping})^2 \right]^{1/2} + \left[ (x_b - \hat{x}_{recept})^2 + (y_b - \hat{y}_{recept})^2 + (z_b - \hat{z}_{recept})^2 \right]^{1/2} \right\} + \Delta t_r + w_k \quad (7)$$

In general, a time of flight is buffered by the acoustic ranging system and made available for processing after a preset timeout following the ping time. The vehicle's estimated state at that time is  $\hat{X}_{k/k}$ . The prediction step being applied first, the vehicle predicted state is  $\hat{X}_{k+1/k}$ . Since the state prediction does not modify the current components and the speed bias estimates, these estimates are constant from the ping time to the time of flight processing time. The vehicle's position is then back propagated in time using the current state and the inputs, which were memorized since the ping. Since the ping time ( $t_{ping}$ ) is known and the reception time ( $t_{recept}$ ) can be calculated by adding the time of flight to the ping time, the position of the vehicle at the ping and at the reception of the reply can then be calculated by:

$$\begin{cases} \hat{x}_{ping} = \hat{x}_{k+1/k} - \sum_{i=t_{ping}}^{t_{k+1/k}} [c\theta_i c\psi_i (u_i - \hat{d}u_{k+1/k}) + \hat{v}_{cnk+1/k}] \Delta t \\ \hat{y}_{ping} = \hat{y}_{k+1/k} - \sum_{i=t_{ping}}^{t_{k+1/k}} [c\theta_i s\psi_i (u_i - \hat{d}u_{k+1/k}) + \hat{v}_{ce k+1/k}] \Delta t \\ \hat{z}_{ping} = \hat{z}_{k+1/k} + \sum_{i=t_{ping}}^{t_{k+1/k}} S\theta_i (u_i - \hat{d}u_{k+1/k}) \Delta t \\ \hat{x}_{recept} = \hat{x}_{k+1/k} - \sum_{i=t_{recept}}^{t_{k+1/k}} [c\theta_i c\psi_i (u_i - \hat{d}u_{k+1/k}) + \hat{v}_{cnk+1/k}] \Delta t \\ \hat{y}_{recept} = \hat{y}_{k+1/k} - \sum_{i=t_{recept}}^{t_{k+1/k}} [c\theta_i s\psi_i (u_i - \hat{d}u_{k+1/k}) + \hat{v}_{ce k+1/k}] \Delta t \\ \hat{z}_{recept} = \hat{z}_{k+1/k} + \sum_{i=t_{recept}}^{t_{k+1/k}} S\theta_i (u_i - \hat{d}u_{k+1/k}) \Delta t \end{cases} \quad (8)$$

### 4.3. Equations of the filter

The filter equations are different from the classical equations in that inputs  $U_k=(\psi, \theta, u)^t$  can be found both in the state and the observation equations. Equations (6) and (7) can be rewritten:

$$\begin{cases} X_{k+1} = f(X_k, U_k) + v_k \\ Z_k = h(X_k, U_k) + w_k \end{cases} \quad (9)$$

The filter proceeds in two steps. The first step is a prediction of the state based on the inputs in  $U_k$ . It basically corresponds to dead reckoning using the last estimates of the underwater current. The state is predicted together with its prediction error covariance  $P_{k+1/k}$ :

$$\begin{cases} X_{k+1/k} = f(X_{k/k}, U_k) \\ P_{k+1/k} = F_k P_{k/k} F_k^T + J_k C_{in} J_k^T + Q_k \end{cases} \quad (10)$$

The second step takes place when a time of flight is available. The predicted state is corrected based on the information carried by the new measurement. The prediction error covariance matrix  $P_{k+1/k+1}$  is also computed:

$$\begin{cases} X_{k+1/k+1} = X_{k+1/k} + K_{k+1} (Z_{k+1} - h(X_{k+1/k}, U_k)) \\ P_{k+1/k+1} = P_{k+1/k} - K_{k+1} (H_{k+1} P_{k+1/k} + S_{k+1}^T) \end{cases} \quad (11)$$

The following Jacobian matrices have to be calculated:

$$\begin{aligned} F_k &= \left. \frac{\partial f(X, U)}{\partial X} \right|_{\substack{X=X_{k/k} \\ U=U_k}}, & J_k &= \left. \frac{\partial f(X, U)}{\partial U} \right|_{\substack{X=X_{k/k} \\ U=U_k}}, \\ H_{k+1} &= \left. \frac{\partial h(X, U)}{\partial X} \right|_{\substack{X=X_{k+1/k} \\ U=U_{k+1}}}, & D_{k+1} &= \left. \frac{\partial h(X, U)}{\partial U} \right|_{\substack{X=X_{k+1/k} \\ U=U_{k+1}}} \end{aligned} \quad (12)$$

$S_{k+1} = J_{k+1} C_{in} D_{k+1}^T$  is a correlation term accounting for the fact that inputs are both in the state and the observation equations. Because of this correlation, the expression of the Kalman gain is a little more complicated than usual:

$$\begin{aligned} K_{k+1} &= (P_{k+1/k} H_{k+1}^T + S_{k+1}) \\ & (H_{k+1} P_{k+1/k} H_{k+1}^T + D_{k+1} C_{in} D_{k+1}^T + R + H_{k+1} S_{k+1} + S_{k+1}^T H_{k+1}^T)^{-1} \end{aligned} \quad (13)$$

#### 4.4. Time of flight validation

When a time of flight is available, its validity is first checked by means of the Mahalanobis distance. The innovation and its variance are calculated by:

$$v_{k+1} = T_{k+1} - h(X_{k+1/k}, U_{k+1}) \quad (14)$$

$$\begin{aligned} P_{v_{k+1}} &= H_{k+1} P_{k+1/k} H_{k+1}^T + D_{k+1} C_{in} D_{k+1}^T + R \\ &+ H_{k+1} S_{k+1} + S_{k+1}^T H_{k+1}^T \end{aligned} \quad (15)$$

The time of flight  $T_{k+1}$  is validated and used to correct the predicted state if it passes the following test:

$$v_{k+1}^T P_{v_{k+1}}^{-1} v_{k+1} < \gamma^2 \quad \text{with } \gamma \text{ typically equal } 1.32 \quad (16)$$

## 5. MAXIMIZATION OF THE INFORMATION MATRIX

Before navigating with respect of the beacon, we want to reduce the uncertainty on the state vector. A study of the information matrix similar to that described in [9] showed that the trajectory that maximizes the information (or conversely minimize the estimation error covariance) consists of leaving the beacon on either side of the vehicle so that the vehicle's heading deviates by  $90^\circ$  from the line joining the vehicle and the beacon (the vehicle describes a circle centered at the beacon) [7]. In order to increase the information, we use the following procedure. At the end of

the  $360^\circ$  rotation, the vehicle is commanded to move at  $90^\circ$  with respect to the beacon. When this condition is achieved, the volume of the prediction error covariance ellipsoid is calculated by:

$$C_0 = \sqrt{\det(P)} \quad (17)$$

When a new time of flight is made available and used by the filter, the volume is calculated for the new covariance matrix:

$$C_k = \sqrt{\det(P_{k/k})} \quad (18)$$

The vehicle keeps circling around the beacon until the ratio of  $C_k$  over  $C_0$  is smaller than a preset threshold (function of  $N$ ). The AUV then reaches its first waypoint and starts doing its survey. At this point the vehicle still uses the filter to estimate its position during the survey.

## 6. SIMULATIONS RESULTS

The algorithm described above has been tested in simulation using the simulator of the torpedo-shaped AUV Taipan developed at LIRMM [10]. In the simulation, the current was set so as to have a 0.2 m/s magnitude and a  $60^\circ$  direction. The speed bias was set at 0.2 m/s. In order to simplify the visualization of the tracks, the absolute position of the beacon is subtracted from all the absolute positions. The beacon then appears to be located at (0,0) on the plots. During the initialization phase, the vehicle dead-reckons its displacements between ranges without any knowledge of its absolute initial position. For the plots, however, the dead-reckoned position was initialized by the vehicle's actual initial position. After the initialization, the filter provides the estimated position of the vehicle in  $R_0$ , which is used to steer the AUV so as to leave the beacon at  $90^\circ$ . We present results for two different vehicle tracks. The first track consists of parallel legs (Fig.2). The second track consists of radial legs (Fig.4).

The AUV starts its  $360^\circ$  rotation at the square mark located at about (-200,-200) with an initial heading of about  $135^\circ$ . The dead-reckoned path is a circle (dark line) since the vehicle is not aware of the current. The actual vehicle trajectory is shown by the distorted circle (light line). The ranges measured during the initialization of the radial mission (a ping every second) are shown in Figure 6. Throughout the simulation, the ranges (or times of flight) were simulated so that 20% of them would be spurious, 20% would be affected by a Gaussian noise with a 10m standard deviation, and the remaining would be affected by a Gaussian noise with an 0.5m standard deviation. The 14 ranges selected for the resolution of the least squares optimization are shown as circles with a star inside.

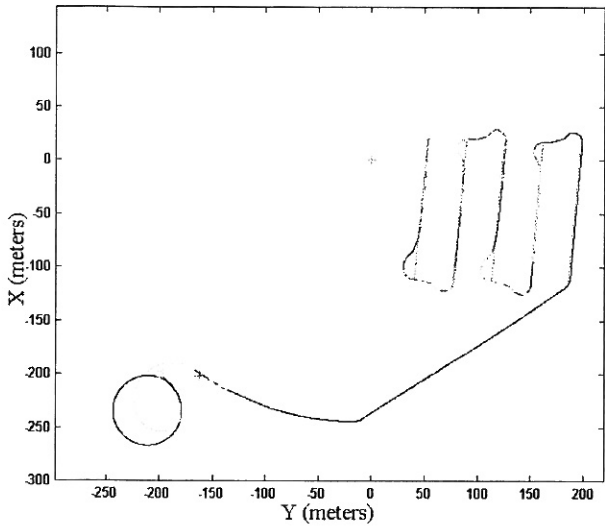


Fig.2: parallel trajectory (dark: estimated, light: actual)

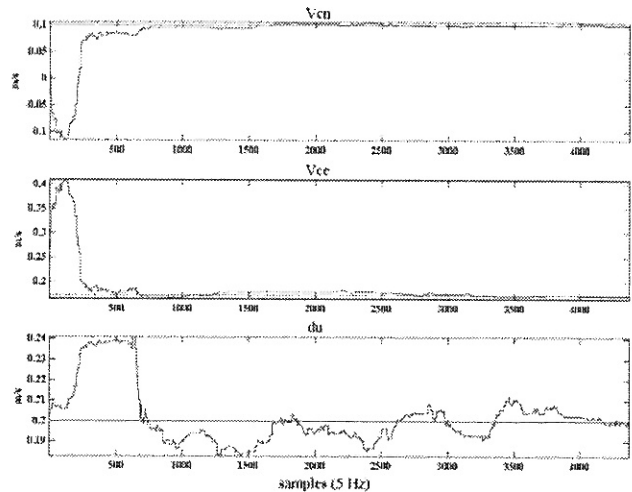


Fig.5: Current and speed bias for the radial trajectory

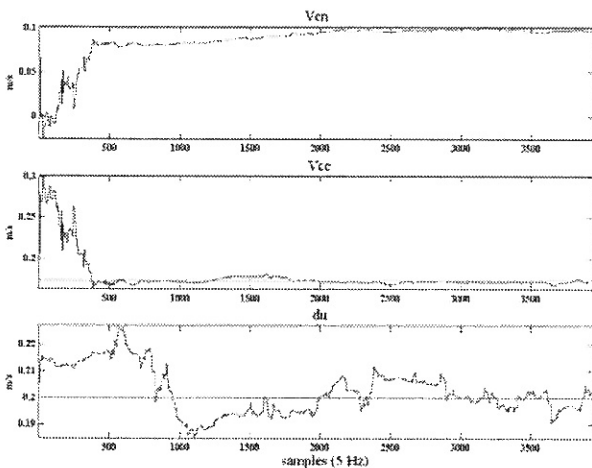


Fig.3: Current and speed bias for the parallel trajectory

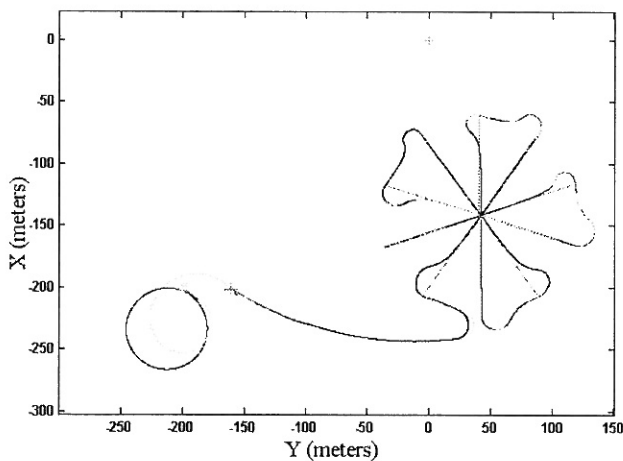


Fig.4: radial trajectory (dark: estimated, light: actual)

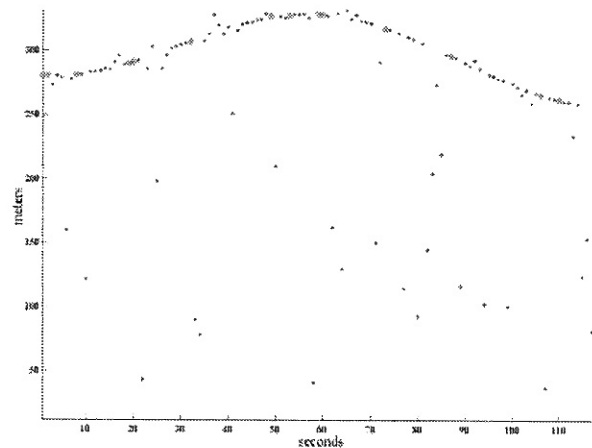


Fig.6: Ranges measured during the initialization of the radial mission

The estimated position of the vehicle at the end of the initialization is shown by a cross at about (-200,-150) in figure 2. It can be seen that this estimated position is very close to the actual position of the vehicle after the distorted circle. The estimated position then jumps from the end of the circle to these coordinates. From there, the actual and estimated trajectories are very close to each other and remain so until the end. The estimates of the underwater current and speed bias components along the runs are shown in figure 3 and 5 (the straight lines show the actual current and speed bias components). It can be seen that the estimates converge to the correct values during the 90° navigation phase. The radial track gives better results principally because of the vehicle travels at varying headings.

## 7. CONCLUSION

In addition to its interest as an alternate solution to classical long baseline, we believe that the range-only solution is worth studying in the more general framework of multiple vehicle operations. Navigation with respect to a beacon by range measurements supposes that the vehicle is able to estimate its position relative to the beacon. If the beacon becomes mobile (carried by another AUV), then the AUV could be able to determine its relative position exactly in the

same way, provided that the beacon can transmit its depth and displacements to the AUV by acoustic communications. Assuming clock synchronization between multiple AUVs, it is then possible to consider having a master vehicle that would ping and transmit its displacements and have the other AUVs determine their position relative to the master AUV.

It has been shown in [7] that this algorithm can also be used to home on a beacon of unknown coordinates.

The simulation results presented in this paper were obtained using the simulator of the Taipan AUV developed at LIRMM (Fig.7). An acoustic modem (Fig.8) incorporating a range measurement capability to a beacon has recently been integrated in Taipan, with the objective of experimenting the algorithm. The vehicle with the acoustic modem transducer is shown in figure 7. In addition to the modem, the vehicle is fitted with a pressure sensor, pitch rate and yaw rate gyrometers, a DGPS, a magnetic compass, a pitch and roll inclinometer. The vehicle speed is based on a priori propeller rpm / speed calibration, so that estimation of the underwater current is critical.

In comparison with long baseline navigation, this method is better in a lot of points : the implementation into play of considerable resources can be avoiding (one beacon against 3 with long baseline), no calibration, less expensive (you need only one range sensor), allows externs parameters estimations (north and east current) without any specific sensors, you can also estimate your own error (speed biases). In opposition, you must realize a specific initialization (maneuvers and lost of time) before beginning a mission.

## REFERENCES

- [1] J.A. Cestone, R.J. Cyr, G. Roesler, and E.St. George, "Recent developments in acoustic underwater navigation", *The Journal of Navigation*, vol.3, n°2, pp. 246-280, May 1977.
- [2] J.G. Bellingham, T.R. Consi, U. Tedrow and D. Di Massa, "Hyperbolic acoustic navigation for underwater vehicles: implementation and demonstration", *Proceedings of the 1992 symposium on Autonomous Underwater Vehicle Technology*, June 2-3, Washington, DC, USA.
- [3] D.K. Atwood, J.J. Leonard, J.G. Bellingham, and B. A. Moran, "An acoustic navigation system for multiple vehicles", *9th Int. Symp. on Unmanned Untethered Submersible Technology*, pp.202-208, New Hampshire, September 25-27, 1995.
- [4] J. Vaganay, J.G. Bellingham and J.J. Leonard, "Comparison of fix computation and filtering for autonomous acoustic navigation", *International Journal of Systems Science*, vol.29, n°10, pp. 1111-1122, 1998.
- [5] A. Matos, N. Cruz, A. Martins and F.L. Pereira, "Development and implementation of low-cost LBL navigation system for an AUV", *OCEANS '99 MTS/IEEE. Riding the Crest into the 21<sup>st</sup> Century*, volume 2, pages 774-779.
- [6] A.P. Scherbatyuk, "The AUV positioning using ranges from one transponder LBL", *OCEANS '95 MTS/IEEE. Challenges of Our changing Global Environment. Conference Proceedings.*, Volume 3, pages 1620-1623
- [7] J.Vaganay, P. Baccou, B. Jouvencel, "Homing by acoustic ranging to a single beacon", *OCEANS '00 MTS/IEEE, Conference and Exhibition, Proceedings Volume 2*, pages 1457-1462, September 11-14, Providence, RI, 2000.
- [8] M.B. Larsen, "Synthetic long baseline navigation of underwater vehicles", *OCEANS '00 MTS/IEEE, Conference and Exhibition, Proceedings Volume 3*, pages 2043-2050, September 11-14, Providence, RI, 2000.
- [9] J. S. Feder, J. J. Leonard, C. M. Smith, "Adaptive mobile robot navigation and mapping," *Int. Journal of Robotics Research, Special Issue on Field and Service Robotics*, July 1999.
- [10] J.Vaganay, B. Jouvencel, P. Lepinay, R. Zapata, "An AUV for very shallow water applications", *World Automation Congress, Anchorage, Alaska, USA*, May 10-14, 1998.

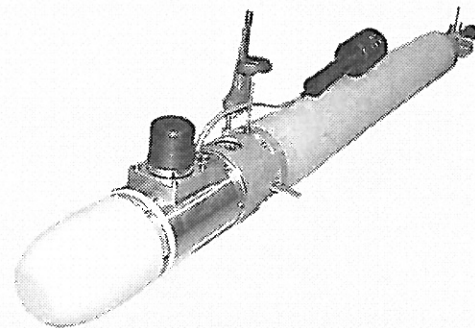


Fig.7: Taipan (length: 1.8m, diameter: 15 cm, weight: 30 kg)

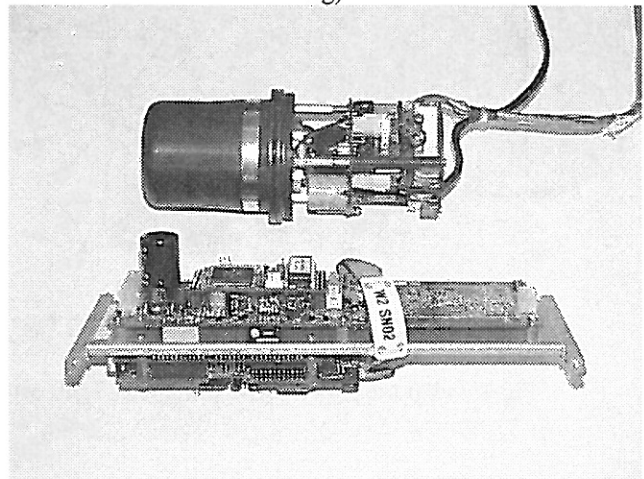


Fig.8: Taipan with the acoustic modem transducer.